DETECTION OF SONAR INDUCED MEASUREMENT UNCERTAINTIES IN ENVIRONMENTAL SENSING: A CASE STUDY WITH THE TOROIDAL VOLUME SEARCH SONAR

CHRISTIAN de MOUSTIER[1] AND TIMOTHY C. GALLAUDET[2]

Marine Physical Laboratory, Scripps Institution of Oceanography,
8602 La Jolla Shores Dr., La Jolla CA 92037-0205, USA

Shallow water field measurements of ocean volume and boundary acoustic backscatter, made with the US Navy`s 68 kHz Toroidal Volume Search Sonar (TVSS), are used to demonstrate the benefits and side effects of a synoptic 360° vertical viewing field with 120 beams at 3° increments when investigating the spatial and temporal variability of the environment. Boundary backscatter measurements can help identify and quantify uncertainties introduced by the sonar system, thus setting realistic bounds on the spatial and temporal scales of environmental features that can be detected with this multibeam sonar. However, acoustic energy reflected at the boundaries and received in the vertical sidelobes of beams steered in the ocean volume often masks finer volume acoustic reverberation features from scattering layers of zooplankton or resonant micro-bubbles. In such cases, a 3 dimensional image built from a sequence of pings along the sonar`s track has proven effective in discriminating sonar induced apparent acoustic variability from environmental variability. A multisector and multi-frequency transmission scheme is proposed to minimize boundary sidelobe interferences.

1 Introduction

Studies of shallow water acoustic variability strive to describe the underlying physical and environmental factors causing the observed variability against which a probability of target detection is sought. Passive sonar measurements rely on discrete spatial and temporal changes in the environment to establish a detection threshold, whereas active sonar measurements rely on disruptions of presumed propagation paths to infer environmental processes at work and the likelihood of target detection. However, assuming that a sound source transmits repeatable and stable acoustic signals somewhere in the water column, the resulting time series of acoustic energy received at hydrophone arrays, co-located with the source or some distance away, will be a combination of reflection and scattering at the sea surface and seafloor boundaries and in the ocean volume, along multiply interfering paths that are often difficult to resolve even when either or both the transmitter and the receiver are directional arrays.

Present addresses: (1) Center for Coastal and Ocean Mapping, Chase Ocean Engineering Lab, University of New Hampshire, Durham, NH 03824-3525, USA, E-mail: cpm@ieee.org; (2) LCDR Tim Gallaudet, Operations Department, USS Kitty Hawk CV-63, FPO AP 96634-2770.

N.G. Pace and F.B. Jensen (eds.), Impact of Littoral Environmental Variability on Acoustic Predictions and Sonar Performance, 571-577.

The high spatial resolution of the multi narrow-beam sonar geometry might seem to be a reasonable choice to reduce such multipath interferences. However, we shall show that this geometry introduces its own set of ambiguities that can be mistaken for environmental acoustic variability. We illustrate this point with quasi monostatic acoustic backscatter measurements made by the US Naval Surface Warfare Center: Coastal Systems Station (CSS), Panama City, Florida, during engineering tests of the Toroidal Volume Search Sonar (TVSS). This sonar operates at 68 kHz with two adjacent and co-axial horizontal cylindrical arrays, each 0.53 m in diameter [1]. One is a 32 element projector array meant to produce a toroidal beam 3.7° wide fore-aft and omni-directional in the sonar's roll plane. The other is a 120 element hydrophone array used to form 120 beams at 3° increments in the roll plane [2].

The tests took place in the northeastern Gulf of Mexico, in about 200 m of water depth, over a nearly featureless sandy silt bottom [3,4], and in sea state 1.5 [4]. For the data considered here, the sonar was towed at 78 m depth, 735 m astern a vessel moving at about 4 m/s. Acoustic propagation conditions were controlled by the sound speed vs. depth profile shown in Fig. 1, and the position of the sonar in the water column yielding the monostatic multipath geometry also shown in the figure.

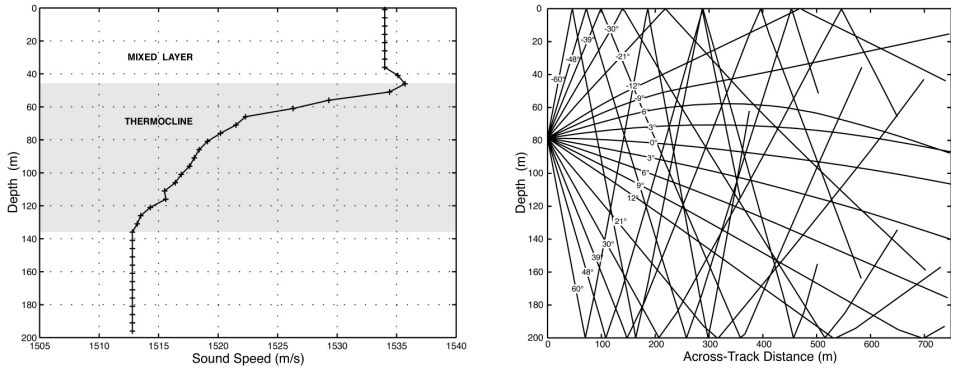

Figure 1. Acoustic propagation conditions at the test site about 120 km southwest of Panama City, Florida: Sound speed profile and rays traced from the 78 m tow depth of the sonar.

In the following we show how the TVSS's 360° multibeam imaging capability for environmental sensing and target detection applications can be strongly biased by sonar induced interferences masquerading as variability in the ocean volume. To minimize these limitations, we propose a multisector transmission geometry with distinct acoustic frequencies for each sector, similar to that used in some modern multibeam swath bathymetry sonars [5], but covering the full 360°.

2 Environmental sensing with the TVSS

The benign environmental conditions at the test site made it possible to highlight the spatial and temporal characteristics of acoustic imagery obtained with the TVSS. For example, an image of average volume acoustic backscattering strength in polar coordinates of elevation angle θ and slant range R from the sonar ($S_v(\theta,R)$), was

obtained from 97 successive pings recorded during a straight run of the sonar at constant depth, by stacking and averaging echoes received in each of the 120 beamformed and roll compensated sectors covering 360° in the roll plane (Fig. 2) [6]. With a 1 Hz ping rate and 4 m/s tow speed, this corresponds to averaging over roughly 400 m along track, thus emphasizing volume acoustic backscatter "features" that remain coherent from ping to ping over that distance.

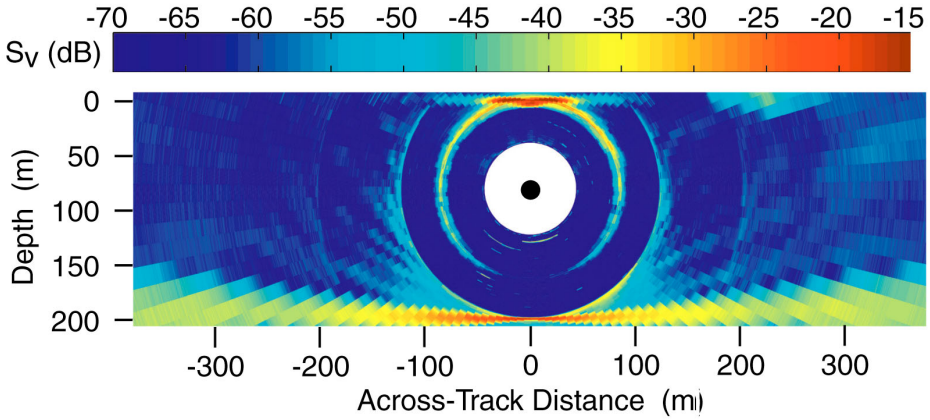

Figure 2. Vertical slice of volume acoustic backscattering strength ($S_v(\theta,R)$) measured in the roll plane of the TVSS (black dot in center of picture) and averaged along track over 97 pings. Echo digitization and recording started at the outer boundary of the central white zone.

In this image, all the beams have the same –3 dB widths of 4.9° (θ_r) in the roll plane and 3.7° (θ_p) in the pitch plane, and they are equally spaced at 3° increments in the roll plane. The transmitted signal is a CW pulse with a bandwidth W of 4.4 kHz. Therefore, with a nominal sound speed C of 1500 m/s, the theoretical volume of a resolution cell for a single ping is given by:

$$\begin{aligned} V(R) &= 2/3\ \theta_p\ \sin(\theta_r/2)\ ((R+C/2W)^3 - R^3) \quad m^3, \\ &\approx 1/3\ \theta_p\theta_r\ ((R+C/2W)^3 - R^3) \quad m^3,\ \text{for } \theta_r < \pi/9 \end{aligned} \tag{1}$$

Hence, for receive beam widths of 20° or less, the resolution cell's volume is directly proportional to the fore-aft transmit beam width and the athwarships receive beam width of the sonar. However, the effective volume of the resolution cell will most likely be somewhat larger than predicted by Eq. (1) because it will depend also on the density, size and aspect ratio of scatterers in each cell [7].

Notable environmental features in Fig. 2 include boundary returns with high volume scattering strength, a small near-surface target visible in two beams at about 210 m horizontal range, a bubble layer from the ship's wake extending 6-8 m below the surface, and biological scattering layers near 45 m depth (more detailed views and analyses of these features are available in refs. [4,6]). Returns from the sea surface are strongest in a ±30° sector, centered on zenith, that corresponds to scattering by resonant micro-bubbles generated in the towing vessel's wake. Observable coherent acoustic

backscatter from the sea surface extends to ±45° about zenith and is also due to the ship's wake which exhibits remarkable persistence over time and space. In fact, the small near-surface target, with a volume scattering strength of 25 dB above ambient noise, is due to micro-bubbles from the decaying wake of the ship on a previous parallel track 200 m away [4]. By contrast, bottom returns exhibit a characteristic angular dependence with high backscatter near nadir dropping rapidly by about 20 dB at 15° incidence and leveling off to the edges of the swath shown. Actually, the bottom returns extend beyond the horizontal limits of the plot and cover a sector in excess of ±75° about nadir.

3 Sonar induced variability

Other notable features in Fig. 2 include concentric rings centered at the sonar, and several diagonal lines appearing in the volume with increasing slopes. The two most prominent rings, that are respectively tangent to the sea surface and the bottom, are due to near zenith, respectively nadir, echoes received in the vertical sidelobes of beams pointed in all the other directions. The fainter rings with larger radii are due to similar vertical sidelobe reception of zenith and nadir multiples. The diagonals are also due to sidelobe reception of: (1) the off-nadir bottom echoes for diagonals that appear to originate at nadir on the bottom and remain tangent to that first bottom sidelobe ring, and (2) off-nadir surface-bottom multiples for the steeper diagonals that appear tangent to the next larger ring with radius of about 200 m.

The importance of these artifacts becomes clear when one considers looking for targets or monitoring environmental variability in the water column contained between 120 m and 200 m horizontal range in Fig. 2. Because of the strong angular dependence of near-specular seafloor acoustic backscatter for most sediments [8], changes in bottom relief might eliminate the sidelobe interference or shift its location in the water column over a number of pings, introducing 8–12 dB of variability in the volume backscatter strength measurements that are unrelated to the spatial characteristics of the volume environment.

The beams displayed in Fig. 2 were formed with a resampled Dolph-Chebyshev amplitude shading window [9] for a uniform -30 dB sidelobe reduction. This technique produces the narrowest mainlobe for a given sidelobe reduction level, and the uniform level of its sidelobes facilitates artifacts detection thanks to their common arrival time in all the beams [10]. However more aggressive sidelobe reduction is obviously needed, but the required amplitude shading windows would increase substantially the width of the mainlobe (e.g. > 60% for raised cosine windows with –60dB sidelobe reduction) [11–13], and increase the volume of the resolution cells in the same proportion (Eq. (1)). To reduce sidelobe interference without sacrificing spatial resolution requires a different transmission paradigm as will be discussed in Sect. 4.

With the toroidal transmission pattern in the roll plane of the TVSS, and the subsequent 360° synoptic view of volume acoustic backscatter afforded by its receiver's multi-narrow beam geometry, one can form a 3 dimensional image of the acoustic field over successive pings. Similar 3 dimensional acoustic visualizations, though not with multibeam sonars, have been used effectively in zooplankton patchiness studies (e.g. [14]). In the case of the TVSS, the 3D image has proven useful to identify region of the water column that are free of sidelobe interference [4,6]. One such region is the

horizontal slice, shown in Fig. 3, which was taken at 4.7 m depth between 40 m and 140 m horizontal range between the first surface and second bottom induced sidelobe rings (Fig. 2).

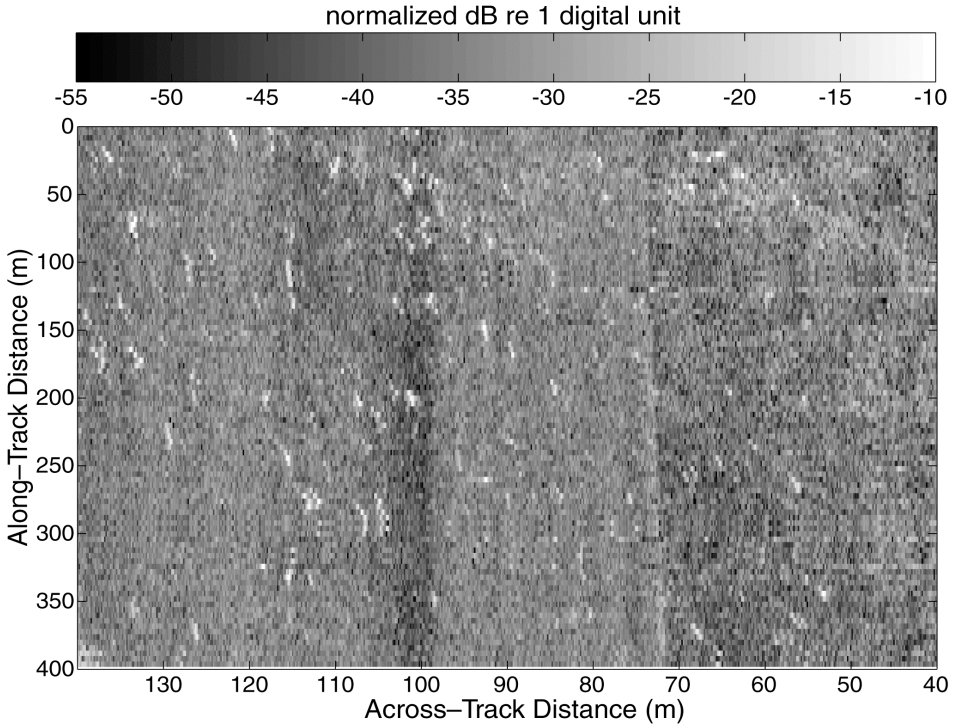

Figure 3. Raster image of a horizontal slice of volume acoustic backscatter 4.7 m below the sea surface. The sonar moves from top to bottom on the right side of this image.

The light features distributed diagonally across the image are most likely due to near surface resonant bubble clouds generated by the wake of the towing vessel. They are 10–15 dB above the background reverberation level, however this background is obscured by along-track bands of pixels with lower volume backscattering strength than their neighbors, resulting from incomplete normalization for the transmit beam pattern.

This illustrates another aspect of multibeam imaging with a sonar whose toroidal transmit beam is not truly uniform. In fact, the TVSS's transmit beam had scallops as deep as 10 dB in the roll plane. Because this transmit beam is not compensated for the instantaneous roll of the sonar, an unnecessary expense for a true toroidal pattern, the highs and lows of the actual transmit beam pattern roll with the sonar and introduce a wavy uncertainty in the volume backscatter data that could affect its statistical analysis (e.g. [15–18]). This uncertainty can only be detected by plotting the data as shown in Fig. 3. Then correction techniques similar to those that have been effective in seafloor acoustic backscatter imagery (e.g. [20,21]) must be applied before any sort of statistical analysis.

4 Multisector transmit geometry

The sidelobe interference patterns shown in Fig. 2 could be reduced substantially, without compromising the volume cell resolution, by modifying the transmit geometry from a toroidal pattern obtained in a single ping to a similar pattern obtained with at least 4 pings transmitted milliseconds apart at different center frequencies in 4 discrete sectors: a 120° sector centered on zenith, a 160° sector centered on nadir and a 120° sector centered on the horizontal on each side of the sonar. The order in which these sectors are transmitted will depend on the position of the sonar in the water column. The volume sectors on either side of the sonar should be transmitted first, using the two lowest center frequencies and the largest source level possible to maximize their range capability. On the other hand, the boundary sectors might require relatively less source level to avoid saturating the receivers with specular surface or bottom backscattering strengths. In addition, the boundary sector with the shortest range should be transmitted last to optimize the ping repetition rate. The four sectors overlap to provide maximum volume coverage individually or combined. However the bandwidths of their transmitted signal should not overlap to maintain good spatial discrimination between the sectors and to avoid inter-sector sidelobe interferences. Real-time roll compensation will be needed during transmit and receive beamforming operations, thus requiring that the sonar's attitude be sampled at about 100 Hz.

5 Conclusions

Applications of the multi-narrow beam sonar geometry are expanding from the now common swath bathymetry usage begun in the mid 1970s, to 3 dimensional imaging of the whole water column as illustrated above. However problem encountered in swath bathymetry (e.g. [19–21]) can be found also, and to a larger extent, in 3 dimensional multibeam imaging. We have used volume acoustic backscattering strength derived from data recorded with the TVSS to show that boundary reflection and scattering can be easily picked up by the vertical sidelobes of beams pointing in the ocean's volume, as well as by non-vertical sidelobes in a multipath environment. Such arrivals could easily be confused for acoustic variability in the medium if a 3 dimensional acoustic image of the water column were not available for inspection prior to statistical analyses of the recorded acoustic reverberation (e.g. [4, 22,23]).

The TVSS was built in the early 1990s and has remained a prototype, but the concept can be generalized to future toroidal sonars provided a different transmission scheme is implemented to avoid boundary sidelobe interference. We proposed transmitting into 4 overlapping sectors, centered respectively at zenith, nadir and on the horizontal, on either side of the sonar. Each sector is assigned a distinct center acoustic frequency and there should be sufficient bandwidth separation between their respective signals to avoid interferences.

Acknowledgments

This work was funded by the US Office of Naval Research under ONR-NRL contract No. N00014-96-1-G913. We wish to thank Maria Kalcic and Sam Tooma (Naval Research Laboratory), CAPT Tim Schnoor USN (ret) (ONR) for their support.

References

1. Volume Search Sonar array program: Preliminary hydrophone test data. Unpublished Tech. Report, Raytheon Co. Submarine Signal Division – Portsmouth RI (1993).
2. McDonald, R.J., Wilbur, J. and Manning, R., Motion-compensated beamforming algorithm for a circular transducer array, *U.S. Navy J. Underwater Acoust.* **47**(2), 905–920 (1997).
3. Stanic, S., Briggs, K.B., Fleischer, P., Ray, R.I and Sawyer, W.B., Shallow-water high-frequency bottom scattering off Panama City, Florida, *J. Acoust. Soc. Am.* **83**(6), 2134–2144 (1988).
4. Gallaudet, T.C., Shallow water acoustic backscatter and reverberation measurements using a 68 kHz cylindrical array, Ph.D. Dissertation, Univ. California San Diego (2001).
5. Kongsberg-Simrad, EM300 & EM120 product descriptions (2001).
6. Gallaudet, T.C. and de Moustier, C., Multibeam volume acoustic backscatter imagery and reverberation measurements in the northeastern Gulf of Mexico, *J. Acoust. Soc. Am*. (in press 2002).
7. Foote, K.G., Acoustic sampling volume, *J. Acoust. Soc. Am.* **90**, 959–964 (1991).
8. APL-UW high frequency ocean environmental acoustics models handbook. Tech. Rep. APL-UW TR 9407, Applied Physics Laboratory – Univ. Washington (1994).
9. Gallaudet, T.C. and de Moustier, C., On optimal amplitude shading for arrays of irregularly spaced or non-coplanar elements, *IEEE J. Oceanic Eng.* **25** , 553–567 (2000).
10. de Moustier, C., Signal processing for swath bathymetry and concurrent seafloor acoustic imaging. In *Acoustic Signal Processing for Ocean Exploration*, edited by J.M.F. Moura and I.M.G. Lourtie (NATO ASI Series – Kluwer, The Netherlands, 1993) pp. 329–354.
11. Sureau, J. and Keeping, K., Sidelobe control in cylindrical arrays, *IEEE Trans. Antennas Propagat.* **30**(5), 1027–1031 (1982).
12. Vu, T.B., Sidelobe control in circular ring array, *IEEE Trans. Antennas Propagat.* **43**(12), 1143–1145 (1993).
13. Mailloux, R.J., *Phased Array Antenna Handbook* (Artech House, Boston, 1994).
14. Greene, C.H., Wiebe, P.H., Pelkie, C., Benfield, M.C. and Popp, J.M., Three-dimensional acoustic visualization of zooplankton patchiness, *Deep-Sea Res. II* **45**, 1201–1217 (1998).
15. McDaniel, S.T., Sea surface reverberation: A review, *J. Acoust. Soc. Am.* **94**, 1905–1922 (1993).
16. Trevorrow, M.V., Vagle, S. and Farmer, D.M., Acoustical measurements of microbubbles within ship wakes, *J. Acoust. Soc. Am.* **95**, 1922–1930 (1994).
17. Medwin H., Acoustic fluctuations due to microbubbles in the near-surface ocean, *J. Acoust. Soc. Am.* **79**, 952–957 (1974).
18. Dahl, P.H. and Plant, W.J., The variability of high-frequency acoustic backscatter from the region near the sea surface, *J. Acoust. Soc. Am.* **101**, 2596–2602 (1997).
19. de Moustier, C. and Kleinrock, M.C., Bathymetric artifacts in Sea Beam data: How to recognize them, what causes them, *J. Geophys. Res.* **91**(B3), 3407–3424 (1986).
20. Hughes-Clarke, J.E., Mayer, L.A. and Wells, D.E., Shallow-water imaging multibeam sonars: A new tool for investigating seafloor processes in the coastal zone and on the continental shelf, *Mar. Geophys. Res.* **18**, 607–629 (1996).
21. Hellequin, L., Lurton, X. and Augustin, J.M., Postprocessing and signal corrections for multibeamechosounder images, *Proc. IEEE Oceans* '97 **,** Vol. 1, 1–4 (1997).
22. Abraham, D.A., Modeling non-Rayleigh reverberation. Rep. SR-266, SACLANT Undersea Research Center, La Spezia, Italy (1997).
23. Middleton, D., New physical-statistical methods and models for clutter and reverberation: The KA-distribution and related probability structures, *IEEE J. Oceanic Eng.* **24**, 261–284 (1999).